УДК [530.12+530.145](082)

ФИЗИЧЕСКИЕ ОСНОВЫ СВОЙСТВА ВОСПРИИМЧИВОСТИ ЭЛЕКТРОМАГНИТНОГО ПОЛЯ ЗЕМЛИ К ГРАВИТАЦИОННО-ВОЛНОВОМУ ИЗЛУЧЕНИЮ ДВОЙНЫХ ЗВЕЗДНЫХ СИСТЕМ

Грунская Л. В.[a,1], Исакевич В. В.[b,2], Исакевич Д. В.[b,3]

[a] Владимирский государственный университет, г. Владимир, 600000, Россия.
[b] ООО Собственный вектор, Владимир, 600005, Россия.

Компоненты вертикальной составляющей напряжённости электрического поля Земли, спектрально локализованные на гармониках частот обращения релятивистских двойных звёздных систем, имеющие значимую амплитуду и большую спектральную локализацию, чем компоненты, локализованные на других частотах, открыты с использованием айгеноскопии (анализа амплитудных спектров собственных векторов матриц смешанных вторых моментов на конечном интервале анализа) на экспериментальном материале многолетних временных рядов напряжённости электрического поля Земли в инфранизкочастотном диапазоне.

Ключевые слова: Собственный вектор, ковариационная матрица, спектральная локализация, электрическое поле Земли, гравитационные волны, релятивистские двойные звёздные системы.

PHYSICAL BASIS OF SENSITIVITY OF THE EARTH'S ELECTROMAGNETIC FIELD TO GRAVITATION

Grunskaya L. V.[a,1], Isakevich V. V.[b,2], Isakevich D. V.[b,3]

[a] Vladimir State University, Vladimir, 600000, Russia.
[b] Eigenvector LLC, Vladimir, 600005, Россия.

Components of the Earth's electric field vertical strength which are spectrally localized at the multiplied rotation frequencies of relativistic binary star systems, have significant amplitude and sharper spectral localization than at the other frequencies, have been discovered at the experimental material of multy-year time series of the Earth's electric field strength in the infralow frequency band using eigenoscopy (second mixed moments eigenvectors' amplitude spectra analysis at finite analysis span).

Keywords: Eigenvector, covariance matrix, spectral localization, Earth electric field, gravitational waves, relativistic binary star systems.

PACS: 04.20.-q
DOI: 10.17238/issn2226-8812.2023.3-4.117-126

Introduction

The task solved in the current work is to reveal the influence of the gravitational waves irradiated by relativistic binary star systems (RBSS) to the Earth electric field vertical strength (E_z).

Components of the electric field vertical strength (in the infralow frequency range and in the near-terrestrial atmosphere layer) which are spectrally localized at the frequencies of the gravitational-wave irradiation from two groups of the RBSS listed in [1]. The first group consists of the small-eccentricity RBSS which have an orbital period from 14 to 207 hours; the expected gravitational waves from a small-eccentricity RBSS are irradiated mainly at the double orbital frequency. The second group consists of

[1]E-mail: grunsk@vlsu.ru
[2]E-mail: eigenoscope@yandex.ru
[3]E-mail: eigenoscope@yandex.ru

Таблица 1. Four time series of vertical component of the Earth's electric field strength in the near-ground layer of atmosphere which have been analyzed

No.	Observation station	Total sample count	Duration, days	Duration, months	Duration, years
1	Voeikovo	170000	7083	236	20
2	Dusheti	120000	5000	167	14
3	Verkhnee Dubrovo	120000	5000	167	14
4	VlSU experimental base	36000	1500	50	4

the high-eccentricity RBSS; the expected gravitational waves from these RBSS are irradiated mainly at the higher multiples of their orbital frequencies.

The conducted research of the electric field components which are spectrally localized at the frequencies of gravitational-wave irradiation from the RBSS are based on the long-time series of the electric field vertical strength at four spatially separated observation stations.

As it is known the Earth-ionosphere resonator has no lower cutoff frequency; therefore all the infralow frequency components of the electric field vertical strength in near-terrestrial layer of the atmosphere, that may be observed at any point of the Earth surface, are formed by the global processes occurring in this resonator. Obviously this resonator may be considered as a part of the Solar system influenced by many factors including the gravitational waves irradiated by RBSS.

Preliminary use of standard spectral analyzers lead to the following result: time series of electric field in the near-terrestrial atmosphere layer are identified by these analyzers as a noise; therefore the gravitational-waves influence of RBSS cannot be revealed with these analyzers.

We've got two choices: the first one is to abandon the problem; the second one (that is our choice) is to solve the problem using some non-standard way of analysis. Following the principle of having a specific analyzer for each problem formulated by L.I. Mandelshtam [2], we chose the way of search of analysis means which should solve a problem of revealing the influence of gravitational waves from RBSS to vertical component of the Earth's electric field strength in the near-ground atmosphere layer.

1. The used data

Four multi-year time series recorded at Rosgidromet observation stations (Voeikovo, Verkhnee Dubrovo, Dusheti) and the Vladimir state university General and Applied Physics Dept. experimental base has been used in the current work. All these time series have the same sampling time equal to 3600 sec; some data about the series is presented in Table 1.

Johnston's list [1] contains 43 small-eccentricity RBSS which irradiate GW at the second multiple of the orbital frequency. These frequencies constitute the first list of frequencies which are used for formation of the multisets' used in the research. This list will be named further as $\lfloor J2F43 \rfloor$. Six RBSS which have high eccentricity have been selected from the Johnston's list for the research at the higher multiples of theirs' orbital frequencies [1]. This list will be named further as $\lfloor JF6/288 \rfloor$. We consider some test multisets of frequencies which are not expected to show the gravitational-wave influence of RBSS on the Earth's electric field; these frequencies are not gravitational-wave frequencies contained in the multisets $\lfloor J2F43 \rfloor$ and $\lfloor JF6/288 \rfloor$ considered for revealing this influence. Among these multisets are multiset of the small-eccentricity RBSS orbital frequencies and of their third multiples; the listed small-eccentricity RBSS does not irradiate gravitation waves of these frequencies. The frequencies close to those listed in Table 2, row 2 are shifted by δF and are not expected to show the gravitational-wave influence.

Таблица 2. The frequency multisets which are used in the current work

No.	Designation	Number of frequencies
1	$\lfloor J2F43 \rfloor$	43
2	$\lfloor JF6/288 \rfloor$	288
3	$\lfloor JF43 \rfloor \oplus \lfloor J3F43 \rfloor$	86
4	$\lfloor JF43 \rfloor \oplus \lfloor J3F43 \rfloor \oplus \lfloor J(F+\delta F)6/288 \rfloor$	374

2. Eigenoscopy of the E_z time series at the selected frequencies

Eigenoscopy provides the following steps:

1. Covariance matrix of the time series is computed with the analysis span of 1000 samples.
2. Eigenvectors and eigennumbers of the covariance matrix are computed.
3. Amplitude spectra and coherence ratios (which is a ratio of the maximum amplitude value to the mean amplitude in the eigenvector amplitude spectrum) of all the eigenvectors are computed.
4. Spectral localization band which is a neighbourhood of main maximum of the amplitude spectrum by 0.707 level is computed.
5. Eigenpairs with spectral localization band containing the frequencies from Table 2 are found.
6. Multisets of coherence ratios and eigenvalues which correspond to the eigenvectors selected at the previous step are formed.

Analysis of statistically significant differences of multisets of coherence ratios and eigenvalues for the frequency multisets No.1 and No.3 have been performed with Bernoulli test (because of a small volume of these multisets). Comparative analysis of cumulative distribution functions for the frequency multisets No.2 and No.4 have been performed with Smirnov-Kolmogorov criterion.

Schemes of eigenoscopes which correspond to these two ways analysis are shown at Figure 1 and Figure 2.

Functional blocks of the eigenoscope scheme are described below.

Block No.1 converts the time series $|s\rangle = |s_1; s_2; \ldots; s_L\rangle$ of L samples to the trajectory matrix $T_{M\times(L-M+1)} = \langle |S_1\rangle, |S_2\rangle, \ldots, |S_{L-M+1}\rangle|$ where $|S_i\rangle = |s_{(i-1)M+1}; s_{(i-1)M+2}; \ldots; s_{i+M-1}\rangle$ is an i-th segment which consists of M consequent samples of the time series; total amount of the segments is $L - M + 1$.

Block No.2 converts trajectory matrix to the density matrix

$$\varrho_{M\times M} = \frac{\sum\limits_{1}^{L-M+1} |S_i\rangle\langle S_i|}{\langle S_i|S_i\rangle} \tag{2.1}$$

Block No.3 computes eigenpairs (eigenvectors and eigennumbers) of the density matrix which are defined by the following relations

$$\langle\psi_i|\varrho_{M\times M} = \lambda_i\langle\psi_i|, i = 1, \ldots, M \text{ in bra form,} \tag{2.2}$$

$$\varrho_{M\times M}|\psi_i|\rangle = \lambda_i|\psi_i\rangle, i = 1, \ldots, M \text{ in cket form.} \tag{2.3}$$

Block No.4 computes amplitude spectra of the eigenvectors. Each of the eigenvectors is extended with $M \cdot U$ zero samples in order to increase spectral discernment. Amplitudes of fast Fourier transform (FFT) are computed for the extended eigenvectors

$$|\mathrm{FFT}(\|\psi_i\rangle; |0_{M\cdot U}\rangle\rangle| = |a_{1,i}; a_{2,i}; \ldots; a_{M(U+1),i}\rangle \tag{2.4}$$

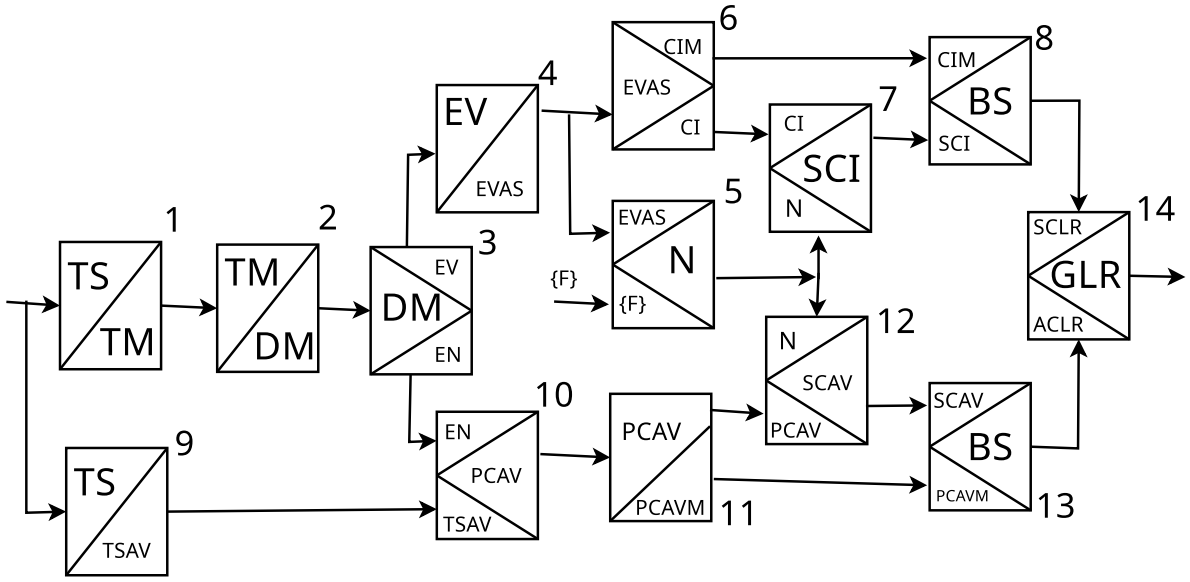

Рис. 1. Eigenoscope (utility models [1–4]): TS — Time series. TM — Trajectory matrix. DM — Density matrix. EV — Eigenvector. EN — Eigennumber. EVAS — Eigenvector amplitude spectrum. CI — Coherence ratio. CIM — Coherence ratio median. SCI — Selected eigenvectors coherence ratios. BS — Bernoulli scheme. SCLR — Spectral channel likelihood ratio. TSAV — Time series active value. PCAV — Principal components active values. PCAVM — Principal components active values median. SCAV — Selected components active values. ACLR — Amplitude channel likelihood ratio. GLR — Generalized likelihood ratio. $\{F\}$ — Frequency list.

First H values of the amplitudes are used as the eigenvectors' normed amplitude spectra estimations:

$$\tilde{A}_i = \frac{|a_{1,i}; a_{2,i}; \ldots; a_{H,i}\rangle}{\max_j a_{j,i}} = |\tilde{a}_{1,i}; \tilde{a}_{2,i}; \ldots; \tilde{a}_{H,i}\rangle \tag{2.5}$$

where H is an integer part of $M(U+1)/2$.

Block No.5 returns the list N_{SEV} of eigenvectors which are spectrally localized near F_j, $j = 1, \ldots, Q$ frequencies is formed in the following way. A set of discrete frequencies (frequency samples)

$$f_i^{(W)} =_{k=1,\tilde{a}_{k,i}>W}^{H} \{k\}, i = 1, \ldots, M \tag{2.6}$$

is defined for each of the normed amplitude spectra $|\tilde{A}_i\rangle$ at which set $\tilde{a}_{k,i}$ exceeds the predefined level W (usually $W = \sqrt{2}$). The upper and lower bounds $f_i^{min} = \min(f_i^{(W)})$, $f_i^{max} = \max(f_i^{(W)})$ of the set $f_i^{(W)}$ are defined and compared with the given discrete frequencies from the list $F_j, j = 1, \ldots, Q$. If the listed frequency lays between the boundaries of $f_i^{(W)}$ then the eigenvector's number is listed at the output of the block. Therefore

$$N_{\mathrm{SEV}} =_{i,j,f_i^{min}<F_j<f_i^{max}} \{i\} \tag{2.7}$$

Further N_{SEV} will mean length of the eigenvectors' list. The lower output of the block No.6 gives coherence ratios for all the eigenvectors. Coherence ratio is computed as a ratio

$$I_i = H \cdot (\sum_{k=1}^{H} a_{k,i})^{?1}, i = 1, \ldots, M \tag{2.8}$$

The upper output is the median value of the coherence ratio

$$I_{\mathrm{med}} = q_{0.5}(I), I = \{I_i\} \tag{2.9}$$

Block No.7 forms set of the coherence ratios for the eigenvectors which are spectrally localized near the frequencies of interest listed in F_j, $j = 1, \ldots, M$. The output set includes coherence ratios of the

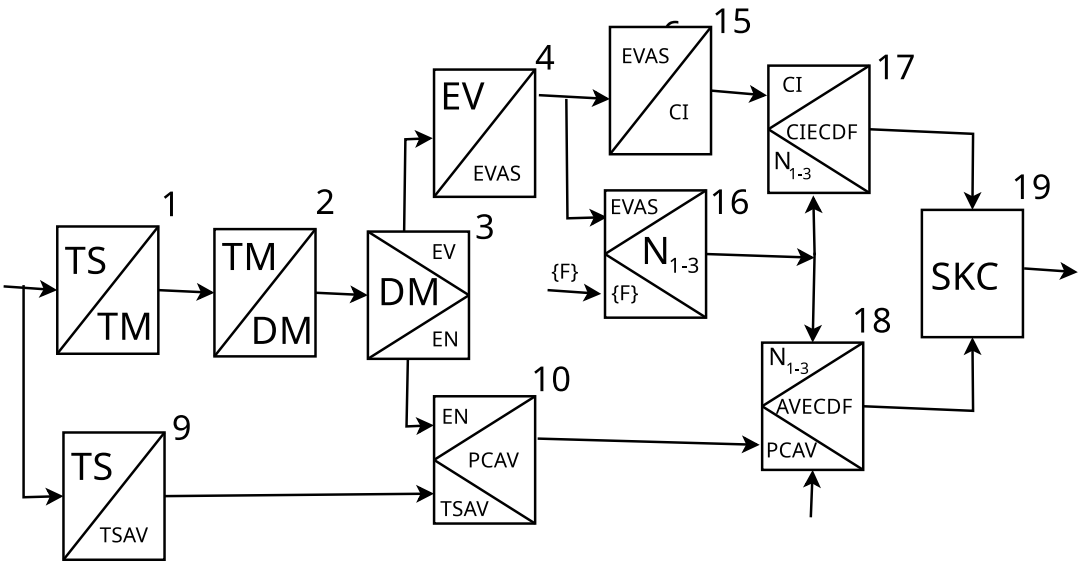

Рис. 2. Eigenoscope used for research at the frequencies of GW from RBSS with high eccentricity (RBSS 6/299 object): TS — Time series. TM — Trajectory matrix. DM — Density matrix. EV — Eigenvector. EN — Eigennumber. EVAS — Eigenvector amplitude spectrum. CI — Coherence ratio. TSAV — Time series active value. PCAV — Principal components active values. SCAV — Selected components active values. $\{F\}$ — Frequency list. CIECDF — Coherence ratios empirical cumulative distribution function. AVECDF — Principal components active values empirical cumulative distribution function. SKC — Smirnov-Kolmogorov criterion. N1-3 — sets of numbers of eigenvectors which are exposed to analysis.

eigenvectors which are listed in N_{SEV}:

$$I_{\mathrm{SEV}} = \{I_i | i \in N_{\mathrm{SEV}}\} \tag{2.10}$$

Block No.8 implements Bernoulli scheme for the spectral processing channel. The Bernoulli scheme works in the following way. Test count $N_{\mathrm{test}} = n(N_{\mathrm{SEV}})$ is equal to the number of selected eigenvectors. Success count $N^{(\mathrm{I})}_{\mathrm{success}} = n(I_i | i \in N_{\mathrm{SEV}} \wedge I_i > I_{\mathrm{med}})$ is equal to number of the coherence ratios of the selected eigenvectors which exceed the median I_{med} of the coherence ratio estimated for all the eigenvectors. Random exceed (success) probability of coherence ratios over the median value is the false detection rate for anomalous spectral localization of E_z near the listed frequencies of GW from RB. This probability is defined as

$$P^{(I)}_{\text{false detection}}(N^{(I)}_{\mathrm{success}}, N_{\mathrm{test}}) = \frac{N^{(I)}_{\mathrm{test}}!}{2^{N_{\mathrm{test}}} N^{(I)}_{\mathrm{success}}! \cdot (N^{(I)}_{\mathrm{test}} ? N^{(I)}_{\mathrm{success}})!} \tag{2.11}$$

while the likelihood ratio is defined as

$$L^{(I)}(N^{(I)}_{\mathrm{success}}, N_{\mathrm{test}}) = \frac{(\lfloor N_{\mathrm{test}}/2 \rfloor)!}{N^{(I)}_{\mathrm{success}}! \cdot (N_{\mathrm{test}} ? N^{(I)}_{\mathrm{success}})!} \tag{2.12}$$

Block No.9 computes the active value D for the time series according to the formula:

$$D = \sqrt{\langle D^2 \rangle}, \langle D^2 \rangle = \frac{\sum\limits_{t=1}^{L?M+1} \langle S_t | S_t \rangle}{M \cdot (L?M + 1} \tag{2.13}$$

Block No.10 computes the active values of the principal components using the time series active value D and the normed eigennumbers λ_i:

$$D_i = \sqrt{\lambda_i} \cdot D \tag{2.14}$$

Block No.11 gives median of the active values of the principal components:

$$D_{\text{med}} = q_{0.5}(D_i) \tag{2.15}$$

Block No.12 gives active values of the principal components which are spectrally localized near the frequencies listed in F_j, $j = 1, \ldots, M$ are defined by the following:

$$D_{\text{SEV}} = \{D_i | i \in N_{\text{SEV}}\} \tag{2.16}$$

Block No.13 implements Bernoulli scheme for the amplitude processing channel works in the following way. The test count for the amplitude channel is the same as for the spectral channel $N_{\text{test}} = n(N_{\text{SEV}})$. The success count is $N^{(D)}_{\text{success}} = n(D_i | i \in N_{\text{SEV}} \wedge D_i > D_{\text{med}})$. The false detection probability of anomalous E_z principal components behavior near the frequencies of GW from RB is defined as

$$P^{(D)}_{\text{false detection}}(N^{(D)}_{\text{success}}, N_{\text{test}}) = \frac{N^{(D)}_{\text{test}}!}{2^{N_{\text{test}}} N^{(D)}_{\text{success}}! \cdot (N^{(D)}_{\text{test}} ? N^{(D)}_{\text{success}})!} \tag{2.17}$$

while the likelihood ratio is

$$L^{(D)}(N^{(D)}_{\text{success}}, N_{\text{test}}) = \frac{(\lfloor N_{\text{test}}/2 \rfloor)!}{N^{(D)}_{\text{success}}! \cdot (N_{\text{test}} ? N^{(D)}_{\text{success}})!} \tag{2.18}$$

Block No.14 according to generalized Bernoulli scheme for the spectral and the amplitude channels for all the reception points gives the following probability

$$P^{(\Sigma)}_{\text{false detection}}(N^{(\Sigma)}_{\text{success}}, N_{\text{test}}) = \frac{N^{(\Sigma)}_{\text{test}}!}{2^{N_{\text{test}}} N^{(\Sigma)}_{\text{success}}! \cdot (N^{(\Sigma)}_{\text{test}} ? N^{(\Sigma)}_{\text{success}})!} \tag{2.19}$$

and likelihood

$$L^{(\Sigma)}(N^{(\Sigma)}_{\text{success}}, N_{\text{test}}) = \frac{(\lfloor N_{\text{test}}/2 \rfloor)!}{N^{(\Sigma)}_{\text{success}}! \cdot (N_{\text{test}} ? N^{(\Sigma)}_{\text{success}})!} \tag{2.20}$$

where

$$N^{(\Sigma)}_{\text{test}} = \sum_g N^{(I)}_{\text{test},g} + \sum_g N^{(D)}_{\text{test},g} \tag{2.21}$$

g is a number of the observation (reception) point. The output of Block No.15 is set of the coherence ratios for all the eigenvectors. The coherence ratio is computed as a ratio

$$I_i = H \cdot (\sum_{k=1}^{H} a_{k,i})^{?1}, i = 1, \ldots, M \tag{2.22}$$

Block No.16 gives lists N_{1--3} which are the lists of eigenvectors' numbers used for further analysis. Set of discrete frequencies (frequency samples)

$$f^{(W)}_i =^{H}_{k=1, \tilde{a}_{k,i} > W} \{k\}, k = 1, \ldots, M \tag{2.23}$$

for which $|\tilde{A}_i\rangle$ exceeds the predefined level W (usually $W = \sqrt{2}$) is defined for each of the normed amplitude spectra $|\tilde{A}_i\rangle$. Lower and upper boundaries $f^{min}_i = \min(f^{(W)}_i)$, $f^{max}_i = \max(f^{(W)}_i)$ of the set $f^{(W)}_i$ are defined which are compared with the discrete frequencies listed in F_j, $j = 1, \ldots, M$. If the frequency lays in the boundaries of $f^{(W)}_i$ then the eigenvector's number is listed at the output. The first output list N_1 is formed as an union of pairs' sets

$$N_1 =_{i,j, f^{min}_i < F_j < f^{max}_i} \{j, i\}, j = 1, \ldots, Q, i = 1, \ldots, M \tag{2.24}$$

The second one (N_2) is formed from N_1 by elimination of pairs with repeated i and extracting the numbers of eigenvectors. The third list N_3 is formed from the numbers of these eigenvectors for which

$f_i^{(W)}$ lays in the multiple RBSS rotation frequencies' range that is the range from $\min_F = \min_{j=1,\ldots,Q} F_j$ to $\max_F = \max_{j=1,\ldots,Q} F_j$.

Coherence ratios' empirical cumulative distribution functions (CIECDFs) are computed for the coherence ratios listed in N_1, N_2 and N_3 correspondingly in Block No.17.

Principal components active values' empirical cumulative distribution functions (AVECDFs) are computed for the active values listed in N_1, N_2 and N_3 correspondingly in Block No.18.

The work of Block No.19 is following. The false detection probabilities are estimated from three CIECDFs using the Smirnov-Kolmogorov criterion. The false detection probabilities are estimated from three AVECDFs using the Smirnov-Kolmogorov criterion. The conclusion on presence or absence of the anomalous behavior of components which are spectrally localized near the frequencies of interest is based on the estimated false detection probabilities.

3. Interpretation of the results

Use of spectral eigenoscopy (which is a signal representation at the finite analysis span using the eigenvectors basis of the signal covariance matrix and the subsequent eigenvectors amplitude spectra analysis) has shown that the Earth electric field vertical strength (measured at the infra-low frequency range) contains non-correlated components; these components are spectrally localized at the gravitational-waves irradiation frequencies of relativistic binary star systems (gravitational-wave beacons) and significantly differ from the other components.

Two groups of the gravitational waves irradiation frequencies are considered in the current article. The first group consists of forty three RBSS having a small eccentricity and an orbital period greater than 14 hours and less than 207 hours. Small eccentricity of the RBSS in this group makes them likely irradiate gravitational waves mainly at their doubled orbital frequencies. The other group consists of six RBSS with high eccentricity and rather long orbital periods (17-231 Earth days); therefore they likely irradiate gravitational waves mainly at higher multiples of their orbital frequencies; total count of the considered multipled frequencies for these RBSS is 288.

Four long (multy-year) time series of the observed Earth electric field strength vertical projection in the infra-low frequency range have been processed in order to get the results; these time series are recorded at the corresponding observation stations Voeikovo, Verkhnee Dubrovo, Dusheti and at the experimental ground of the General and Applied Physics Department, Vladimir state university.

Non-correlated components of all these time series have been examined. Properties of the non-correlated components spectrally localized at the two groups of the considered gravitational wave frequencies differ from the corresponding properties of the non-correlated components spectrally localized at the other frequencies; the difference is statistically significant.

The results of the article make it possible to affirm that there is no reason to negate a gravitational-wave influence of the RBSS to the Earth electromagnetic field. The authors suppose that observation of the Earth electromagnetic field components at the RBSS gravitational-wave irradiation frequencies may start a multi-frequency gravitational-waves monitoring; this new direction of research may reveal new opportunities for research of the Earth and Universe.

The current research is made possible because previously was made the following [5, 6, 7, 8, 9, 10, 11]:

1. Found out that classical methods of spectral analysis do not reveal anomalies of the Earth electromagnetic field amplitude spectra at the RBSS gravitational-wave frequencies.

2. Found out that adding small harmonic components with the RBSS gravitational-wave frequencies to the observation time series leads to a sure detection of these components using the classical spectral analysis.

3. Fixed the absence of harmonic components at the gravitational-wave frequencies in the time series of Earth electric field vertical strength in the near-terrestrial atmosphere layer.

4. Found out that the searched signal is not harmonic but is a signal of unknown structure which is spectrally localized near the gravitational-wave frequency of RBSS.

5. Found out (by theoretical estimation) that tidal effects in the Earth atmosphere caused by the RBSS gravitational wave influence may cause only the vanishingly small variations of the Earth electric field vertical strength. As a result, a question arose about the other possible mechanisms of RBSS gravitational-waves influence on the electric field vertical strength in the near-terrestrial layer of atmosphere.

6. Performed an experimental study of using the covariance matrix eigenvectors basis for analyzing the Earth electric field vertical strength time series. It appeared that the analyzer using such a representation was not studied specially.

7. Introduced a special class of signal eigenvectors and components analyzers (eigenoscopes) to theory and practice. Set a task of eigenoscope properties systematic study and consolidating the priority for the use of this class of analyzers in the form of patents.

8. Performed the study of eigenvectors and eigennumbers typologies (behavior) for regular oscillations and stochastic signals depending on the source signal, the finite analysis span and the way of forming the observations ensemble.

9. Performed the study of eigenoscopes supersensitivity and superselectivity effects compared to the classical amplitude and energetic spectra analysis methods. Estimated the eigenoscopy precision depending on the quantization noise and the properties of the analyzed signal.

10. Developed the criteria of eigenvector spectral localization and of eigenvectorsamplitude spectra closeness to the RBSS gravitational wave irradiation frequencies. Estimated false detection probability.

11. Used Bernoulli test and Smirnov-Kolmogorov criterion to develop effective rules of statistical inference on abnormal behavior of the non-correlated components (eigenpairs) at the RBSS gravitational-wave irradiation frequencies.

12. Showed that for the Earth electric field vertical projection strength the observed rms values (more than 0.1 V/m) of non-correlated components spectrally localized at the RBSS gravitational waves irradiation frequencies may be explained using a theory of the Earth orbital perturbations caused by the RBSS gravitational waves; these perturbations lead to the Earth shift in relation to total charge of the atmosphere (in the ionosphere-terrestrial resonator).

13. Proved the existence of spatial (between the spatially separated observation stations) correlations of non-correlated components spectrally localized near the RBSS gravitational-waves frequencies.

The results of this work are based on the observation data of the Earth electric field donated by Y. M. Schwartz (Voeikovo, Verkhnee Dubrovo, Dusheti stations); on the data recorded at the experimental ground of Department of General and Applied Physics of Vladimir State University (lead by L. V. Grunskaya); on the RBSS list published by Johnston at his site [1] and on the innovative processing methods (called eigenoscopy) [3]. The results does not contain any explanations of the observed effects; though simple estimations [10] allow the assumption that the observed effects are the result the RBSS gravitational waves influence on the Earth-Sun gravitational antenna. Due to the different degrees of this influence on the Earth and on its atmosphere the observed effects may caused by the relative shift of the total storm charge in the global ground-ionosphere resonator.

Conclusion

Significant (false detection probability is less than 10^{-9}) difference of eigenvectors' coherence ratios and normed eigenvalues for the eigenvectors which are spectrally localized at the small-eccentricity RBSS double orbital frequencies (using Bernoulli test) and which are spectrally localized at the higher multiples of the high-eccentricity RBSS orbital frequencies (using Smirnov-Kolmogorov criterio) from those of the test multisets have been revealed.

It is known that: eigennumbers spectrum of the E_z covariance matrix is similar to the one of covariance matrix of a partially-integrated noise; while the eigenvectors of it are spectrally localized near frequencies which are lowered with the eigennumber growth [5].

Also it is shown that a small perturbing monochromatic component which is spectrally localized at a given frequency and added to the partially integrated noise leads to a significant perturbation of the components with small eigennumbers without significant change of the dominant components if spectral localization of the perturbation is higher than of the noise. Pair of eigenvectors is observed the spectral localization of which is similar to spectral localization of the perturbation [12].

These two facts may explain the sensitivity of E_z to perturbations from RBSS GW which show itself in the higher spectral localization of the covariance matrix' eigenvectors spectrally localized at the frequencies of interest.

Список литературы/References

1. http://www.johnstonsarchive.net/relativity/binpulstable
2. Gorelik G.S. L. I. Mandelshtam i uchenie o rezonanse *Akademik L. I. Mandelshtam k 100-letiyu so dnya rozhdeniya*. Moscow, Nauka, 1979, pp.138–157.
3. Isakevich V.V., Isakevich D.V., Grunskaya L.V., R. F. Utility Model Patent No. 116,242 (30 September 2011).
4. Isakevich V.V., Isakevich D.V., R. F. Utility Model Patent No. 178, 399 (28 June 2017).
5. Isakevich D.V., Grunskaya L.V. *Russian Physics Journal* 2015, 58, pp. 1160–1166.
6. Grunskaya L.V., Isakevich V.V., Isakevich D.V., Lukyanov V.E. *Russian Physics Journal* 2017, 59, pp. 1373–1379.
7. Grunskaya L.V., Isakevich V.V., Isakevich D.V. *Gravitation and Cosmology* 2018, 24, pp. 384–392.
8. Grunskaya L.V., Isakevich V.V., Isakevich D.V. *Russian Physics Journal* 2019, 62, pp. 55–61.
9. Grunskaya L.V., Isakevich V.V., Isakevich D.V. *Russian Physics Journal* 2020, 63, pp. 34–42.
10. Grunskaya L.V., Isakevich V.V., Isakevich D.V. *Russian Physics Journal* 2021, 64, pp. 496–503.
11. Grunskaya L.V., Isakevich V.V., Isakevich D.V. *Russian Physics Journal* 2022, 65, pp. 440–449.
12. Grunskaya L.V., Isakevich V.V., Isakevich D.V. *Materials of IX All-Russian Scientific Conference on the Atmospheric Electricity* 2023, pp. 65–74.

Авторы

Грунская Любовь Валентиновна, д.т.н., профессор, Владимирский государственный университет, ул. Горького, д. 87, г. Владимир, 600000, Россия.
E-mail: grunsk@vlsu.ru

Исакевич Валерий Викторович, к.т.н., доцент, ООО Собственный вектор, ул. Горького, д. 50, г. Владимир, 600005, Россия.
E-mail: eigenoscope@yandex.ru

Исакевич Даниил Валерьевич, ООО Собственный вектор, ул. Горького, д. 50, г. Владимир, 600005, Россия.
E-mail: eigenoscope@yandex.ru

Просьба ссылаться на эту статью следующим образом:
Грунская Л. В., Исакевич В. В., Исакевич Д. В. Физические основы свойства восприимчивости электромагнитного поля Земли к гравитационно-волновому излучению двойных звездных систем. *Пространство, время и фундаментальные взаимодействия.* 2023. № 3-4. С. 117–126. **Authors**

Grunskaya Liubov Valentinovna, Ph.D., Professor, Vladimir State University, Gorkogo st., 87, Vladimir, 600000, Russia.
E-mail: grunsk@vlsu.ru

Isakevich Valery Victorovich, Ph.D., Associate Professor, Eigenvector LLC, Gorkogo st., 50, Vladimir, 600005, Russia.
E-mail: eigenoscope@yandex.ru

Isakevich Daniil Valeryevich, Eigenvector LLC, Gorkogo st., 50, Vladimir, 600005, Russia.
E-mail: eigenoscope@yandex.ru

Please cite this article in English as:
Grunskaya L. V., Isakevich V. V., Isakevich D. V. Physical Basis of Sensitivity of the Earth's Electromagnetic Field to Gravitation. *Space, Time and Fundamental Interactions*, 2023, no. 3-4, pp. 117–126.